J.Natn.Sci.Foundation Sri Lanka 2012 ***40****(3):211-219*

RESEARCH ARTICLE

Tsunami wave loading on buildings: a simplified approach

K.M.K. Bandara and W.P.S. Dias*
Department of Civil Engineering, Faculty of Engineering, University of Moratuwa, Moratuwa.

Revised: 05 April 2012 ; Accepted: 04 May 2012

Abstract: The simplest way to express the magnitude of a tsunami load is based on its wave height or depth of inundation at a given location. This paper aims to discuss such a simple but realistic tsunami loading scheme and a dynamic analysis method to evaluate a given structure. A case study of a reinforced concrete framed building is used to demonstrate how this can be done. The total tsunami load is expressed as a combination of different components that have particular distributions with respect to time and space. These are applied on the 2D reinforced concrete frame from the case study and both static and dynamic time history analysis were performed to quantify tsunami damage in terms of hinge formation. It is shown that the impulsive force is the critical component of the tsunami load. The suggested total tsunami load is $2.5\ \rho g h^2$ per unit width, where h is the depth of inundation.

Keywords: Dynamic analysis, hinge formation, impulsive force, tsunami loading.

INTRODUCTION

The Indian Ocean tsunami and its devastating effects on lives, infrastructure and the economy (Dias *et al.*, 2006) have raised questions as to what could be done to prevent or minimize such a level of loss in the future. A major requirement towards this approach is the ability to predict the wave magnitudes, arrival times to shorelines, and the consequent inundation levels. Another requirement is the ability to design structures that are less vulnerable to tsunami damage. Extensive research into both numerical and physical modelling, varying from deep-ocean propagation to shallow-water and onshore aspects of the waves, have achieved the first target to a certain extent (Dalrymple *et al.*, 2006). With respect to the second, namely, structural aspects, one should be able to predict the loads that will be experienced by structures due to tsunami waves and the structural responses due to such loading. There are several modern finite element techniques, such as volume-of-fluid and level set methods, which allow water surface tracking in Eulerian models; and Lagrangian particle methods, such as MPS (moving particle semi-implicit) and SPH (smoothed particle hydrodynamics) that can be used with a structural solver to perform coupled fluid-structure interaction analysis. Physical modelling in wave tanks provides an alternative to the finite element analysis approach mentioned above and has been used by several researchers (Arikawa, 2006; Thusyanthan & Madabhushi, 2008) in studying structural aspects associated with tsunamis. However, both approaches require many resources, consume much time and effort, and yield results that are case dependent and are effective only in providing conceptual suggestions or in examining a specific case in detail. They cannot be incorporated into the design process in a simple manner to evaluate a given structure against tsunami loading.

The overall aim of this study was to propose a simple but realistic loading scheme and a dynamic analysis method to evaluate structures against tsunami loading - one that can be incorporated into the design process if required, as opposed to numerical fluid-structure interaction modelling or physical modelling in wave tanks. This study follows initial work undertaken by Dias and Mallikarachchi (2006).

METHODS AND MATERIALS

In this study, the relevant information available in literature is presented and a simple loading scheme to represent the various components of tsunami loads on structures is proposed. Then the case of a two storey school building, typical of those that survived the tsunami waves was investigated. The structural performance of this reinforced concrete framed building during the

* Corresponding author (priyan@uom.lk)

tsunami was examined using the proposed tsunami loading scheme. Both static and dynamic time history analysis were performed using the commercial structural analysis software SAP2000. The case study was used to judge the loading scheme proposed earlier by comparing the actual performance of the building with results from the analysis. This was compared with the conservative Japanese approach (Okada *et al.*, 2005) of using an equivalent hydrostatic force corresponding to a depth of 3 times the inundation depth as the tsunami load.

Components of tsunami loading

Velocity: Velocity is one of the major properties of tsunami loading. By and large, velocity is taken as depending on the inundation depth, h. The expression for the velocity is $u = k\sqrt{(gh)}$. Different authors give different values for k (Murty, 1977; Kirkoz, 1981; FEMA, 2000a; Iizuka & Matsutomi, 2000; Thurairajah, 2005).

The velocity obtained by $k = 2$ corresponds to the classical solution of the leading tip of a surge on a frictionless horizontal plane generated by a dam break with the quiescent impoundment depth of h. However, it is argued (Yeh *et al.*, 2005) that this may be too crude, because the computed tip velocity does not represent the velocity of a flow depth h; therefore, this equation is not appropriate to represent the flow velocity for a tsunami flood passing through a structure. At the same time Bryant (2001) reported that velocities in between 5.9 and 9.3 m/s can be obtained from a tsunami wave height of 8 m. If $k = 1$ is used for $h = 8$ m in the above equation, the velocity is obtained as 8.9 m/s, which is quite close to Bryant's upper limit. Hence it is reasonable to conclude that it is sufficient to use $k = 1$ in the velocity equation.

Hydrostatic pressure: Hydrostatic pressure occurs when standing or slowly moving water encounters a building or a building component. Hydrostatic loads can act laterally on an object. This load always acts perpendicular to the surface to which it is applied. If a structure or structural element is surrounded by water, it is the difference in inundation heights on opposite faces that will result in net horizontal force.

In most cases, the hydrostatic pressure has been considered as ρgh, where ρ is the fluid density. Thus the pressure is a function of inundation depth (h) only. As noted before, Japanese practice (Okada *et al.*, 2005) takes a $3\ h$ deep hydrostatic force as the total tsunami force, which is equal to $4.5\ \rho gh^2$ per unit width. In this paper, ρgh is used as the maximum static pressure; this is a triangularly distributed pressure for a height of h, that results in a static load of $0.5\ \rho gh^2$ per unit width.

Hydrodynamic pressure: When water flows around a building or a structural element at a moderate to high velocity, hydrodynamic loads are applied to the building. These loads are functions of flow velocity and the structure geometry, and include frontal impact on the upstream face, drag along the sides and suction on the downstream side. They are usually called drag forces, and are a combination of the lateral loads caused by the impact of the moving mass of water and the friction forces as the water flows around the obstruction.

The common equation (Thurairajah, 2005) for the dynamic pressure is $0.5C_d\ \rho u^2$. Here, C_d is the drag coefficient and u is the velocity. Most authors have stated that C_d is 2.0 for rectangular columns or piles and 1.2 for circular ones. For large rectangular buildings, C_d values vary from 1.25 to 2.0 depending on the ratio of the width of building to the inundation depth (FEMA, 2000a). The pressure distribution is uniform, except for FEMA-55 (2000a), which states that if the wave velocity is less than 3.0 m/s, the distribution will be triangular. If we use $u = \sqrt{(gh)}$, based on evidence from Bryant (2001) as discussed earlier and $C_d = 2.0$ for a rectangular column, which is our element of interest, the pressure then becomes $0.5\ C_d\rho u^2 = 0.5 \times 2 \times \rho \times gh = \rho gh$. The distribution will be uniform over a height of h.

Impulsive pressure: The major difference between a tsunami and a normal flood is that the tsunami has an impulsive action. It occurs suddenly with a considerable force but ceases in a comparatively short period. Thus, the tsunami load may be very high but it will be short lived.

Thurairajah (2005) has provided some details on impulsive pressure. According to him, at the flood level the impulsive pressure is $1.5\ \rho gh$ and decreases to $0.5\ \rho gh$ at the base and zero at a height of h above the flood level. According to Nakamura (1974), the impulsive pressure is $0.5\ C_t\ \rho u^2$, where $C_t = 3$ for 45^o and 1.8 for 22.5^o, the angles being the wave tip inclinations. If we take $C_t = 3$ and $u = \sqrt{(gh)}$, then the pressure becomes $1.5\ \rho gh$; but Nakamura (1974) has not defined its distribution.

Thus, an approach similar to Thurairajah (2005) was used in this study. The pressure was varied above the inundation depth from ρgh to zero at a height of h above the inundation level. This can be taken as transient hydrostatic pressure of the wave run up to a height of h above the inundation depth. The pressure below the inundation depth was taken as a constant value of $0.5\ \rho gh$. When the uniform hydrodynamic pressure of ρgh was added to this pressure, we obtained a total pressure of $1.5\ \rho gh$, equal to the pressure suggested by

Nakamura (1974). The three components of tsunami loading described above are depicted in Figure 1.

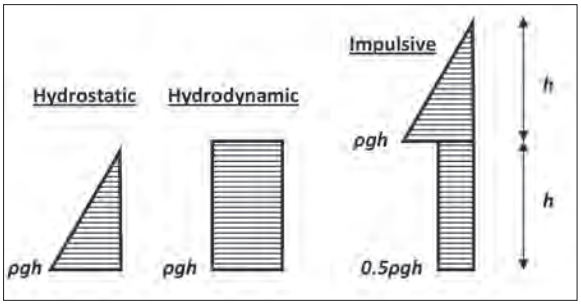

Figure 1: Proposed tsunami pressure components

Other forces: Waves breaking directly onto structures can cause large breaking forces, but these will occur only on very steep slopes and hence are not considered here. Impact forces that arise from debris impact can either be computed (FEMA, 2000a), or their effect is determined by studying the effect of losing various supporting elements in turn [see also work by Madurapperuma and Wijeyewickrema (2008)]. When building elements are submerged, buoyancy forces can be accounted for by using submerged densities.

Total pressure: Instead of using various load types in combination, equations for total pressure or force are available in literature. The Japanese approach of using a hydrostatic force corresponding to a depth of 3 times inundation depth is based on the work of Okada *et al.*, (2005), who have defined the total pressure as *(3h-z) ρg*. Asakura *et al.* (2000) have introduced two equations for the total pressure. Without soliton break up, the total pressure is *(3h-z)ρg,* exactly the same as in Okada *et al.* (2005); but when there is soliton break up, the total pressure changes to *max[(5.4h-4z),(3h-z)]ρg.* Here *z* is the height from the ground level to the point at which the pressure is calculated.

Recent work by Thusyanthan and Madabhushi (2008) suggests that the maximum wave loading on housing can be as high as 10 –12 times the hydrostatic load, higher than even the guidelines in the Japanese approach (Okada *et al*., 2005). Other experimental work reported in that study appear to indicate still larger factors. However, many such researchers have used fairly high velocities in comparison to inundation depths, in fact much higher than reflected by $u = \sqrt{(gh)}$, and this may be the cause for such unrealistic results.

Thurairajah (2005) has stated that the pressure should be reduced by 40 % if the zone of wall under consideration has more than 30 % of openings, with linear interpolation applicable for lower percentages of openings.

Loading history: Tsunami loads are very high in magnitude but act for rather short durations, i.e they are time varying loads. Therefore, the loading history should be determined but most researchers have not focused on this.

Arikawa (*Personal communication, 2006*) has carried out model studies in a wave flume, which gives an idea of loading history. A rather high pressure is experienced within the first second of impact and after that there is a decay to a lower value (called a "standing pressure"), which is sensibly constant for nearly 8 s. Then the load decays and disappears within the next 6 s.

The above loading history was used for the case study in a rather simple manner. If the element under consideration for load application becomes completely inundated by water, the hydrostatic load quickly becomes zero. Thus, it is reasonable to assume that the hydrostatic load also follows the same loading history as the impulsive load in such a situation - in fact the hydrostatic load also acts impulsively. Hence, it can be assumed that the initial peak above the standing pressure occurs due to impulsive and hydrostatic forces. The hydrodynamic force will act constantly for the standing pressure duration and then decay to zero.

Case Study

Description of the selected building: The two storey school building selected for the case study (Figure 2) was subjected to a 3 m height of inundation, a common phenomenon during the 2004 tsunami in Sri Lanka. All such buildings survived the lateral loading from waves. In a few cases there was localized damage following the complete undermining of end columns due to scour, but that is a different phenomenon altogether.

The long way direction has 9 bays of 3.1 m each. The upper floor beams and roof beams (both of cross section 525 x 225 mm) span 7.5 m in the short way direction and are supported on columns (of cross section 225 x 225 mm) that run along the two long way edges. Since the wave forces were applied in the more critical short way direction of the building, a typical internal frame (Figure 3) was considered sufficient to study the phenomena. It should be noted that a loading width of 3.1 m is used only for dead loads while tsunami loads are calculated based on pressure acting across the column

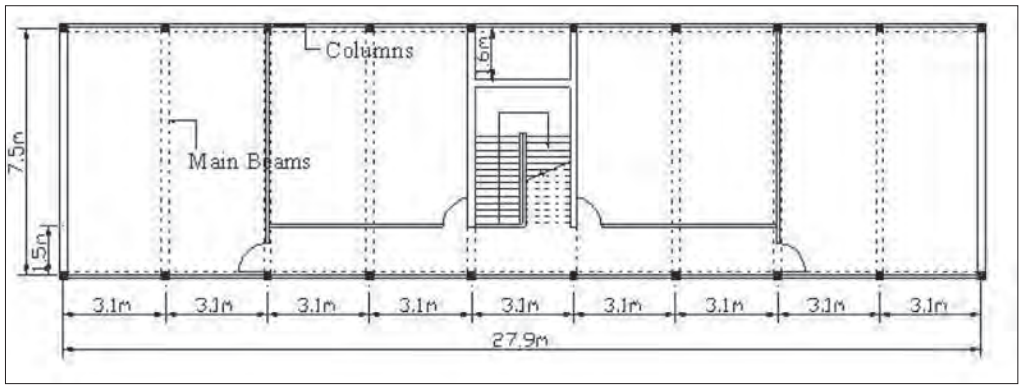

Figure 2: First floor plan of the case study building

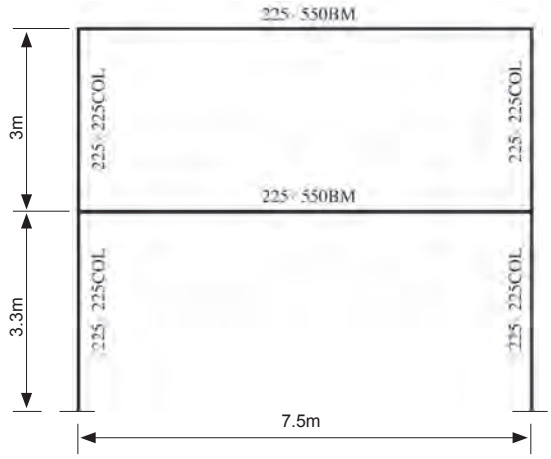

Figure 3: Internal frame from the case study

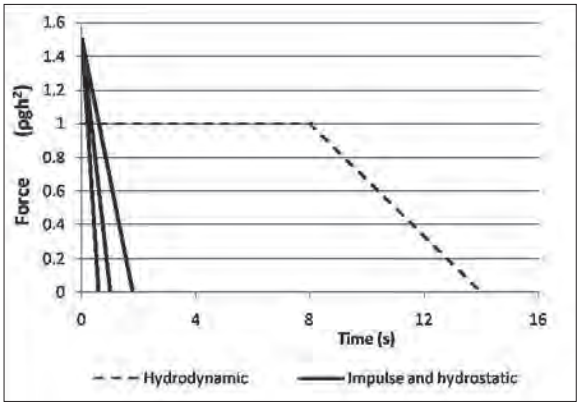

Figure 4: Time history functions of the load components

width only, given that the long way edges have only low non-structural walls.

Applied loading: Only the 3 relevant load types were used in this study (shown in Figure 1), namely:

1. Hydrostatic load (total of $0.5\ \rho gh^2$ per unit width)
2. Hydrodynamic load (total of ρgh^2 per unit width)
3. Impulsive load (total of ρgh^2 per unit width)

All tsunami loads act simultaneously for the static analysis, but for the dynamic analysis the time history function as depicted in Figure 4 was used. The hydrodynamic load will stay constant for 8 seconds and will gradually decrease to zero within the next 6 seconds; this follows Arikawa (*Personal communication, 2006*). It was discussed earlier that the impulsive load acts within the first second. However three impulse durations of 0.6 s, 1.0 s and 1.8 s were used in order to study the effects of this variation. The hydrostatic load was assigned the same time history function as the impulsive load, as discussed earlier.

The total maximum load was $2.5\ \rho gh^2$ per unit width, or 5 times the hydrostatic load. It should be noted that this is valid only for rectangular column type structures, which however are the most common. This can be compared with non-dimensionalized results (Figure 5) reported by Arikawa (*Personal communication, 2006*), where the maximum load is 4.25 times the hydrostatic load (of $0.5\ \rho gh^2$). It should be noted that Arikawa (2009) has reported much higher forces too. Nevertheless, it can

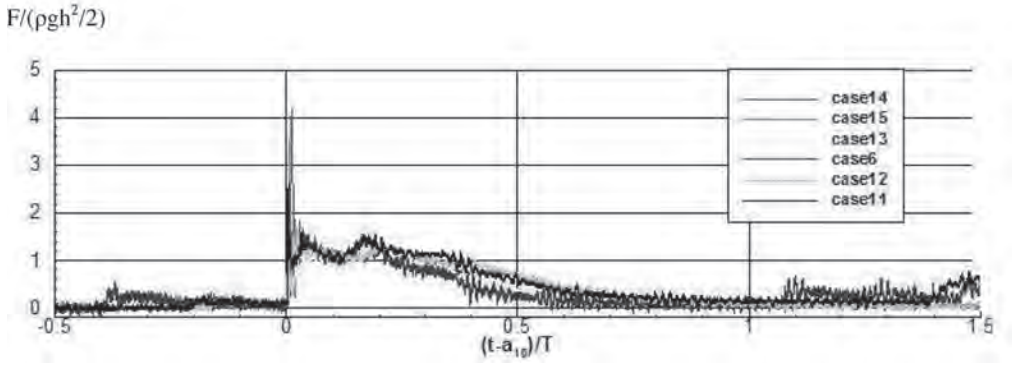

Figure 5: Non-dimensionalized load history reported by Arikawa (*Personal communication, 2006*)

be concluded that estimation of tsunami loads in this study is reasonable. Note that this is considerably less than the value obtained using the conservative Japanese approach (Okada *et al*., 2005) that gives a total load of $4.5\ \rho gh^2$ per unit width (over an assumed inundation depth of 3 *h*) and thus 9 times the hydrostatic load corresponding to the inundation depth *h*. This large load was also applied as a static load on the model and was defined as Case A. Case B corresponds to the reduced total load of $2.5\ \rho gh^2$ per unit width advocated in this paper (Figure 4), while in Case C the distributions in Figure 4 were scaled up so that a total load of $4.5\ \rho gh^2$ per unit width was obtained. This was for comparison between the recommended Japanese hydrostatic load and a more nuanced load combination with 3 load types but the same total load.

In addition to the tsunami loading described above, the first floor slabs were assumed to carry a distributed load of 1 kN/m^2 (only furniture and finishes) and the roof beams, a distributed load of 0.6 kN/m^2. These loads were kept unfactored, as were the tsunami loads.

Model definition: Grade 20 concrete was specified, as used in the actual school building, and an E value of 24.6 kN/mm^2 was used in the model as calculated from the grade according to BS 8110 (1997), but without the material safety factor γ_m. A nonlinear material model was used with the above E value, a Poisson ratio of 0.2 and a concrete compressive strength of 20 N/mm^2. The actual reinforcement present in the building is specified in the relevant element properties that are used for defining the hinges (i.e. 4T16 with R6 @150 for columns).

Hinges were assigned to the frame (Figure 6) at locations where high member forces were expected; tsunami loads were applied from left to right. Note that PMM hinges (axial load plus moments about other 2 axes) are defined for columns and M3 hinges (moments about 3 axes) are defined for the beams. SAP2000 implements the plastic hinge properties described in FEMA-356 (2000b). As shown in Figure 7, five points labelled A, B, C, D, and E define the force–deformation behaviour of a

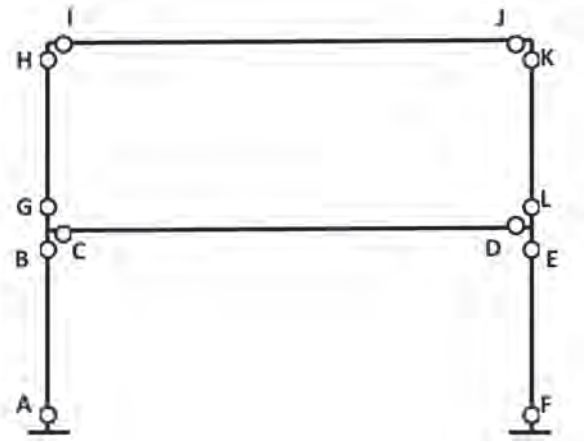

Figure 6: Locations of hinges

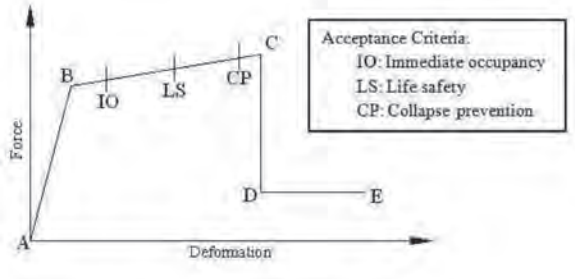

Figure 7: Load deformation behaviour of a plastic hinge

plastic hinge. The values assigned to each of these points vary depending on the type of the element, material properties, longitudinal and transverse steel content, and the axial load level on the element.

Since hinge formation is available only for nonlinear analysis, direct integration time history analysis was used, because the modal superposition methods only yield linear analysis results. It is very difficult to verify manually whether the results of a time history analysis are correct or not. The method adopted here was to scrutinize the base shear values obtained for abnormalities due to different input values such as time step and damping. The importance of using an adequately small time step was clear from Figure 8, which showed that the hinge formation is completely missed when a time step of 0.1 s was used. The similarity of results for time steps of 0.01 s and 0.001 s implies that the former is adequate for this situation. Making a correct estimation of damping is another important issue in dynamic analysis, as it not only affects structural response but also numerical convergence. Some numerical trials indicated that proportional damping of 5 % for both stiffness and mass would yield good results. The widely adopted Hilber-Hughes-Taylor method was used in this work with zero numerical damping.

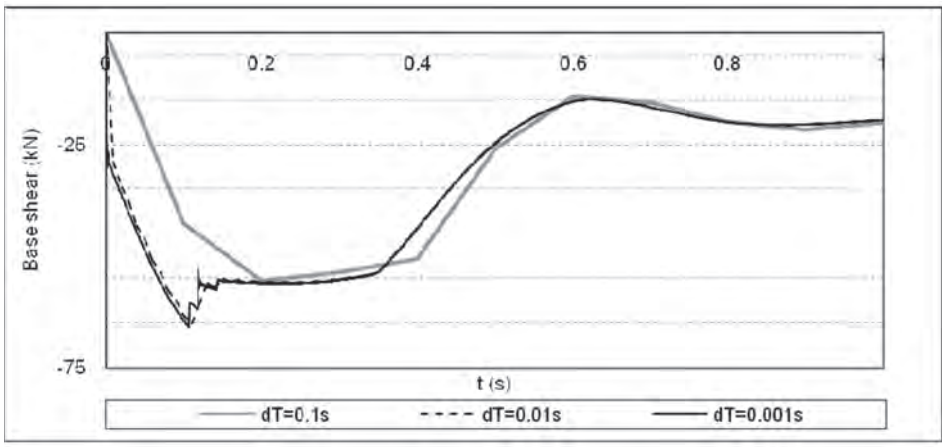

Figure 8: Base shear from using different time step sizes

RESULTS AND DISCUSSION

Hinge formation and collapse

From the two load Cases B and C that correspond to total tsunami loads per unit width of $2.5\ \rho gh^2$ and $4.5\ \rho gh^2$ respectively, a significant hinging was not evident in Case B, in both static and dynamic analyses. The sudden change in the base shear due to hinging during dynamic analysis can be seen in Figure 9 for Case C (for 1 s impulse duration). The maximum deflection values shown in Table 1 also reflect this, while hinge formation in Case B, evident in Table 2 is only minor as the plastic rotation values are very small. However Case B is on the threshold of significant hinging for an impulse duration of 1.8 s (Table 2). Case A has resulted in full collapse due to excessive rotation at hinges. This raises the question about the Japanese approach (Okada *et al.*, 2005) being too conservative. It should be noted that school buildings of this sort did not fail during the tsunami; neither did they display any distress in the columns or beams of the frames. The actual buildings were of course stiffened by a stair well, and some of them by infill walls within alternate frames too (Figure 2). Nevertheless loadings A and C do seem somewhat excessive and unrealistic. As demonstrated before (Dias & Mallikarachchi, 2006), it should also be noted that the more nuanced dynamic analysis in Case C resulted in a smaller structural response than if the total load was applied as a static load (Case A).

Variations in loading

A change in the time duration of the hydrodynamic load using a constant value for 24 s that decreases to zero in the next 18 s (total duration of 42 s) was tried in

order to explore the sensitivity of the results to changes in these durations. This produced the identical response for the first 8 s, which includes all the critical effects. This leads to the conclusion that it is mainly the impulse time duration that is of critical importance in the loading history.

It is evident that there is more damage to the structure when the impulsive load duration increases from 0.6 s to 1.8 s as observed with maximum deflection (Table 1) and plastic rotation (Table 2) values.

Tsunami wave actions on the rear column, which in fact would also be hit by tsunami waves were also considered. Since the wave velocity is taken as $u = k\sqrt{(gh)}$ with $k = 1$, the time taken for the wave front to travel the distance between the two columns is approximately 1.4 s. Hence, only an impulse duration of 1.8 s will result in an overlap of all three load components acting on the two columns; else only the hydrodynamic components overlap, i.e. if 0.6 s or 1.0 s impulse durations is used. The results in Table 3 reflect this.

Table 1: Maximum deflection (mm) at top of rear upper floor column

Load case (with total load)	Impulse duration 0.6 s	1.0 s	1.8 s	Static
Case A (4.5 ρgh^2)	-	-	-	Full collapse
Case B (2.5 ρgh^2)	9.4	10.2	11.0	8.3
Case C (4.5 ρgh^2)	73.1	198.1	Full collapse	Full collapse

Table 2: Formation of column hinges, locations (Figure 6) and maximum plastic rotation (rad)

Load case (with total load)	Impulse duration 0.6 s	1.0 s	1.8 s	Static
Case A (4.5 ρgh^2)	-	-	-	Full collapse
Case B (2.5 ρgh^2)	E; 0.00043	A,E; 0.00083	A,E; 0.00119	E; 0.00043
Case C (4.5 ρgh^2)	A,B,E,F; 0.0214 (>CP#)	A,B,E,F; 0.0589 (>CP#)	Full collapse	Full collapse

Beyond collapse prevention state (Figure 7); all other hinges are less than the immediate occupancy (IO) state

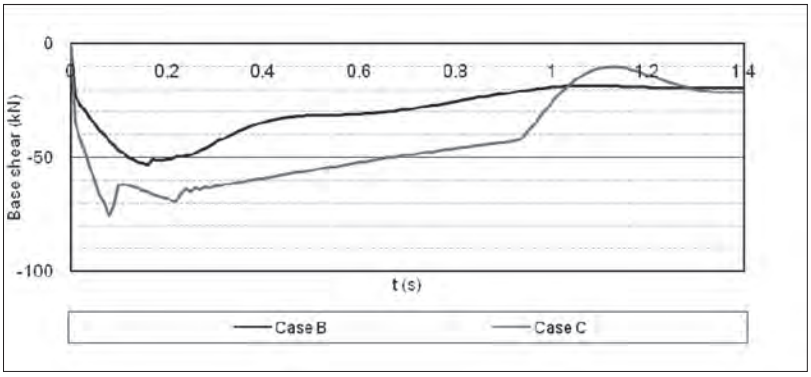

Figures 9: Base shear history for 1 s impulse duration

Table 3: Comparison of using a single impact and dual impact for Case B

	Results with single impact		Results with dual impact	
Impulse duration	Max deflection (mm)	Hinge locations and max plastic rotation (rad)	Max deflection (mm)	Hinge locations and max plastic rotation (rad)
0.6 s	9.4	E, 0.00043	12.9	A, E, F; 0.00283 (>CP#)
1.8 s	11.0	A, E, 0.00119	19.5	A, E, F; 0.00567 (>CP#)

Beyond collapse prevention state (Figure 7); all other hinges are less than the immediate occupancy (IO) state

CONCLUSION

This study indicates that a load of $2.5\,\rho g h^2$ per unit width can be considered a realistic value for the total tsunami load on rectangular columns of a structure. Based on a comparative study of literature, limited experimental evidence, and some support from the case study it could be predicted that significantly higher loads would result in collapse. However, there was no structural damage observed during the tsunami (although the actual buildings were stiffened by stair wells). The total load of $2.5\,\rho g h^2$ per unit width can be considered a lower bound on design tsunami loading. A method of breaking down the total tsunami load into different components has been suggested, once again based on a comparative study of the literature. The influence of the impulsive force component, including its distribution over time, was also clearly seen.

It was shown that dynamic time history analysis can avoid the over-conservative results obtained from a static analysis. The methodology adopted can be used to evaluate a given structure against tsunami loading. It is also simple enough to be incorporated into the design process if necessary.

Acknowledgement

The contributions of H.M.Y.C. Mallikarachchi and H.D. Yapa to preliminary work on this research is acknowledged, as is the funding from the University of Moratuwa (Senate Research Fund), Holcim (Lanka) Ltd. and Finco Engineering Sales Directorate.

REFERENCES

1. Arikawa T. (2009). Behaviours of concrete walls under impulsive tsunami load, *Joint Conference on Earthquake and Tsunami*, Turkish Chamber of Civil Engineers, Ankara, Turkey.
2. Asakura R., Iwase K., Ikeya T., Kaneto T., Fujii N. & Omori M. (2000). An experimental study on wave forces acting on on-shore structures due to overflowing tsunamis. *Proceedings of Coastal Engineering* **47**: 911 − 915 (in Japanese).
3. British Standards Institution (1997). *BS 8110*: *Structural Design of Concrete*. British Standards Institution, London, UK.
4. Bryant E. (2001). *Tsunami: The Underrated Hazard.* Cambridge University Press, London, UK.
5. Dalrymple R.A., Grilli S.T. & Kirby J.T. (2006). Tsunamis and challenges for accurate modeling. *Oceanography* **19**(1): 142 − 151.
6. Dias P., Dissanayake R. & Chandratilake R. (2006). Lessons learned from tsunami damage in Sri Lanka. *ICE Proceedings on Civil Engineering* **159**(2): 74 − 81.
7. Dias W.P.S. & Mallikarachchi H.M.Y.C. (2006). Tsunami – planning and design for disaster mitigation. *The Structural Engineer* **84**: 25 − 29.
8. Federal Emergency Management Agency (FEMA) (2000a). Determining site-specific loads, chapter 11. *FEMA Coastal Construction Manual (FEMA-55)*. Federal Emergency Management Agency, Washington DC, USA.
9. Federal Emergency Management Agency (FEMA) (2000b). *Prestandard and Commentary for Seismic Rehabilitation of Buildings (FEMA-356)*. Federal Emergency Management Agency, Washington DC, USA.
10. Iizuka H. & Matsutomi H. (2000). How to estimate damage due to tsunami flood? *Proceedings of Coastal Engineering* **47**: 381 − 385 (in Japanese).

11. Kirkoz M.S. (1981). Breaking and run-up of long waves. In: Tsunamis: their science and engineering. *10th IUGG International Tsunami Symposium,* Sendai-shi/Miyagi-ken, Japan.
12. Madurapperuma K.M. & Wijeyewickrema A.C. (2008). Nonlinear response of RC buildings due to impact of tsunami water-borne boats and containers. *14th World Conference on Earthquake Engineering*, International Association for Earthquake Engineering, October, Beijing, China.
13. Murty T.S. (1977). Seismic sea waves: tsunamis. *Bulletin of the Fisheries Research Board of Canada No.198*. Fisheries and Marine Service, Scientific Information and Publishing Branch, Department of Fisheries and the Environment, Ottawa, Canada.
14. Nakamura S. (1974). Shock pressure of tsunami surge on a wall. *NOAA-JTRE Tsunami Research Symposium, International Union of Geodesy & Geophysics* **22** : 177 − 185.
15. Okada T., Sugano T., Ishikawa T., Ohgi T., Takai S. & Hamabe C. (2005). *Structural Design Method of Buildings for Tsunami Resistance (SMBTR)*. The Building Centre of Japan, Tokyo, Japan.
16. Thurairajah A. (2005). Structural design loads for tsunami and floods. *International Conference on Disaster Reduction on Coasts*, November, Melbourne, Australia.
17. Thusyanthan N.I. & Madabhushi S.P.G. (2008). Tsunami wave loading on coastal houses: a model approach. *ICE Proceedings on Civil Engineering* **161**: 77 − 86.
18. Yeh H., Robertson I. & Preuss J. (2005). *Development of Design Guidelines for Structures that Serve as Tsunami Vertical Evacuation Sites*. Washington Division of Geology and Earth Resources, Open file report - 4, November, 2005.